

# First-principles prediction of a metastable crystalline phase of Ga with *Cmcm* symmetry

Maurice de Koning, Alex Antonelli, and Diego Alejandro Carvajal Jara  
*Instituto de Física Gleb Wataghin, Universidade Estadual de Campinas - UNICAMP, Caixa Postal 6165,  
 Campinas 13083-970, SP, Brazil*

(Received 17 February 2009; revised manuscript received 9 June 2009; published 24 July 2009)

We report on evidence for the existence of an unknown metastable crystalline phase of gallium by the combination of classical molecular-dynamics (MD) simulations and density-functional theory (DFT) calculations. The MD simulations, based on a modified embedded-atom potential, reveal the unknown crystalline form through a first-order phase transition originating from the *Cmca* symmetric  $\alpha$ -Ga phase under hydrostatic tension. Subsequently, the DFT calculations using two different generalized-gradient approximation functionals are employed to verify its stability and determine its electronic structure. The structure of the orthorhombic phase is described by symmetry group *Cmcm* and shows a dimer arrangement resembling the  $\alpha$ -Ga phase. A first-order phase transition from  $\alpha$ -Ga to the unknown phase is estimated to occur at  $-1.3$  GPa.

DOI: [10.1103/PhysRevB.80.045209](https://doi.org/10.1103/PhysRevB.80.045209)

PACS number(s): 61.50.Ah, 61.66.Bi, 71.20.-b

The element Ga is of fundamental technological importance, being an essential building block in the semiconductor industry. So far, the application of this element has concentrated mostly on its use in compounds such as GaN and GaAs, which are employed in optoelectronic devices. Recently, however, it has been shown that even elemental Ga may be proven useful in a technological context, demonstrating potential as a phase-change material. Such materials have recently become the topic of considerable interest due to their potential application in nonvolatile and low-power electronic memory devices.<sup>1-4</sup> The fundamental property of such systems is that they feature rapid transitions between different phases. While phase-change materials typically feature transitions between a crystalline and an amorphous phase,<sup>4</sup> in the case of Ga it was shown that a nanoparticle can be made to pass through a sequence of four different metastable crystalline phases.<sup>1,3</sup> Accordingly, the potential of elemental Ga as a phase-change material is closely related to our understanding of its phase diagram.

Ga is known to be highly polymorphic, fostered by the coexistence of covalent and metallic bonding types. In addition to the zero-pressure stable  $\alpha$ -Ga (Ref. 5) phase (also referred to as Ga-I) and the liquid or vapor, it contains at least four crystalline phases that are stable at elevated pressure, namely, Ga-II,<sup>5-7</sup> Ga-III,<sup>6</sup> Ga-IV,<sup>8</sup> and Ga-V.<sup>7</sup> Furthermore, there are at least four metastable phases in the low-pressure regime known as  $\beta$ -Ga,<sup>9</sup>  $\delta$ -Ga,<sup>10</sup>  $\gamma$ -Ga,<sup>11</sup> and  $\epsilon$ -Ga,<sup>6</sup> respectively. Curiously, while the latter phase is observed in the phase-change sequence in Ga,<sup>1</sup> its crystal structure and most basic physical properties remain unknown.<sup>6,12</sup> In addition to technological applications, an understanding of this polymorphism is also of importance within the context of the physics of density-driven first-order liquid-liquid phase transitions, for which recent experiments have shown evidence in Ga.

In this paper we present evidence for the existence of an unknown crystalline phase of elemental Ga that is metastable at zero pressure. The evidence is entirely rooted from simulation results, based on a combination classical molecular-dynamics (MD) simulations using the modified embedded-atom model (MEAM) for Ga (Ref. 13) and density-functional-theory (DFT) calculations. After the initial

observation of the unknown phase in a classical MD simulation during which  $\alpha$ -Ga is heated under hydrostatic tension, the structure is then optimized using the DFT approach at zero external pressure and temperature, conditions under which it is found to be metastable. Furthermore, the DFT cohesive energy of the predicted metastable phase is found to be higher than that of all the other known metastable crystalline phases of Ga at conditions of zero pressure.

Figure 1 shows results of the classical MD simulations<sup>14</sup> based on the MEAM potential. The simulations were carried out using a cell containing 1152 Ga atoms initially arranged on the *Cmca*-symmetric  $\alpha$ -Ga lattice. The cell was first equilibrated within the *NPT* ensemble at a temperature of 50 K and a hydrostatic pressure of  $-1.6$  GPa. Subsequently, the system was heated at the same constant pressure of  $-1.6$  GPa, slowly ramping its temperature to 1050 K in  $4 \times 10^6$  MD steps of 1.5 fs each. Figure 1 shows the volume per atom as a function of the instantaneous kinetic temperature. The result clearly shows the occurrence of two abrupt transitions. The first is a transition from the  $\alpha$ -Ga phase to the predicted phase near 690 K, involving an increase in the

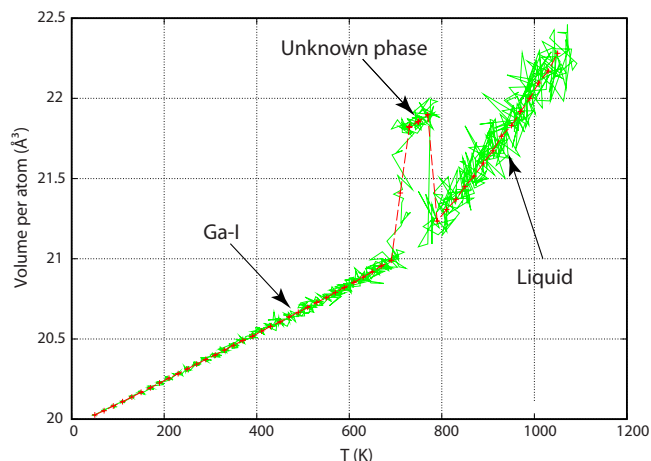


FIG. 1. (Color online) Volume as a function of instantaneous kinetic temperature in the MEAM-based classical MD simulation (full line). Average heating rate is 175 K/ns. Dashed line is a guide for the eye.

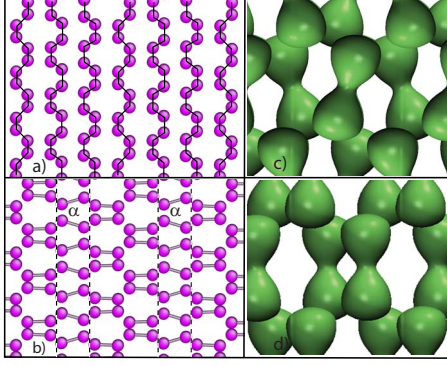


FIG. 2. (Color online) Panels (a) and (b) show atomic configuration after the first transition shown in Fig. 1. The thick lines in panel (a) are shown to guide the eye and distinguish the different wavelike patterns. The dashed lines in panel (b) indicate the positions of the planar faults separating  $\alpha$ -Ga from the unknown structure. The two domains containing the  $\alpha$  phase are indicated by the symbol  $\alpha$ . Panels (c) and (d) display the electronic charge density of the  $\alpha$ -Ga phase and the metastable structure, respectively. Both iso-surfaces correspond to a density of  $0.3e/\text{\AA}^3$ .

atomic volume by almost 4%. Upon further heating, the latter then transforms into the liquid phase at  $T \approx 800$  K.

The identification of the unknown phase as being crystalline is made by conjugate-gradient quenching of a corresponding atomic configuration. The result of the quench is depicted in Fig. 2, which shows a view perpendicular to the  $c$  axis<sup>15</sup> of the original  $\alpha$ -Ga phase. Figure 2(a) shows how the structure can be seen as a succession of wavelike patterns. When considering adjacent “waves,” one observes two possibilities. In one case, neighboring waves are “in phase,” while in the other they are  $180^\circ$  out of phase. The former pattern is characteristic of  $\alpha$ -Ga, whereas the latter reveals a previously unknown structure. The predicted structure also features the presence of Ga dimers. When looking at the configuration of Fig. 2(a) from this point of view, as shown in Fig. 2(b), it is clear that the computational cell obtained after the quench is a mixture of the two phases. There are two domains of  $\alpha$ -Ga and the predicted phase each, separated by four planar defects. The main difference between  $\alpha$ -Ga and the predicted phase is that while in the former case the dimers have alternating orientations, in the latter they are all aligned.

Although the MEAM description predicts the existence of this unknown crystalline phase of elemental Ga, transferability is always an issue when it comes to using semiempirical models of interatomic interaction. Therefore, to verify the robustness of the findings, we subsequently subject the predicted phase to a first-principles study. To this end we employ the state-of-the-art DFT implementation of the Vienna *ab initio* simulation package (VASP),<sup>16–18</sup> using the projector-augmented-wave (PAW) (Ref. 18) approach for both the Perdew-Burke-Ernzerhof (PBE) (Ref. 19) and the Perdew-Wang 91 (PW91) (Ref. 20) generalized-gradient approximations (GGA). We use the PAW potentials treating three electrons in the valence panel, a plane-wave kinetic-energy cutoff of 175.1 eV, and the Methfessel-Paxton integration scheme with a smearing width of 0.2 eV. For  $\alpha$  and predicted phases, calculations are carried for 144- and 8-atom cells, using  $3 \times 3 \times 2$  and  $11 \times 11 \times 7$   $k$ -point meshes, respectively, for converged results. Calculations for the known metastable phases,  $\beta$ ,  $\gamma$ , and  $\delta$ , were carried out using unit cells containing 4, 40, and 22 atoms, respectively. Here,  $k$ -point meshes of  $13 \times 13 \times 7$ ,  $9 \times 7 \times 3$ , and  $7 \times 7 \times 7$  guaranteed the convergence of the results. All configurations were optimized at zero external pressure, adjusting both atomic and cell degrees of freedom. In the final configuration the forces on all atoms were smaller than  $0.001$  eV/ $\text{\AA}$ . All total-energy values were obtained using the tetrahedron integration method with Blöchl corrections.

First, to assess the quality of this computational scheme, we applied it to the  $\alpha$ -Ga phase, for which experimental data<sup>21,22</sup> as well as previous DFT results<sup>15</sup> are available. A summary of the results is shown in Table I (the lattice parameters and the internal coordinates  $u$  and  $v$  are named according to Ref. 15). As discussed earlier,<sup>15</sup> one of the problems of the local-density approximation (LDA) to DFT is the underestimation of the atomic volume and the overestimation of the bulk modulus by  $\sim 10\%$  with respect to the experimental values. The present GGA calculations lead to a significant improvement of the atomic volume, giving a discrepancy of less than 5% for both GGA functionals. The GGA structural parameters are essentially identical to the LDA values and are in good agreement with the experimental data. GGA significantly underestimates the bulk modulus, showing discrepancies of  $\sim 20\%$  compared to the experimental value. On the other hand, the GGA cohesive energies are in

TABLE I. Comparison of structural data for  $\alpha$ -Ga. Theoretical results at zero pressure and temperature. Experimental data correspond to atmospheric pressure and a temperature of 4.2 K. The first five parameters specify the  $\alpha$ -Ga structure as explained in Ref. 15.

Property	LDA (Ref. 15)	PBE-GGA (this work)	PW91-GGA	Expt. (Refs. 21 and 22)
$a$ ( $\text{\AA}$ )	4.387	4.5849	4.5898	4.509
$b/a$	1.0013	1.0016	1.0005	1.0013
$c/a$	1.695	1.695	1.691	1.695
$u$	0.0814	0.0807	0.0814	0.0785
$v$	0.1573	0.1561	0.1561	0.1525
Atomic volume ( $\text{\AA}^3$ )	17.93	20.45	20.45	19.41
Bulk modulus (kbar)	669	494	495	613
Cohesive energy (eV)		2.913	2.936	2.969

TABLE II. DFT-GGA elastic constants of predicted metastable phase (in kbar) for PW91 and PBE functionals, obtained by computing stress tensors resulting from six independent cell distortions. Final column gives values for the bulk modulus  $B$ .

	$C_{11}$	$C_{22}$	$C_{33}$	$C_{44}$	$C_{55}$	$C_{66}$	$C_{12}$	$C_{13}$	$C_{23}$	$B$
PBE	707	717	692	243	304	241	421	79	370	429
PW91	709	770	710	253	303	259	384	119	337	430

good agreement with the experimental values, with discrepancies of less than 2%.

Next, we used the same DFT approaches for the predicted crystalline phase. The calculations were carried out using a supercell that was obtained by cutting an eight-atom orthorhombic periodic cell from the conjugate-gradient-relaxed 1152-atom cell used in the MEAM-based MD simulations. Subsequent relaxation for both GGA functionals, without enforcing any lattice symmetries, reveals that the structural features observed in the MEAM simulations persist. Posterior symmetry analysis of the atomic arrangement reveals that the predicted structure is an orthorhombic phase with  $Cmcm$  symmetry (space group 63). The corresponding equilibrium orthorhombic unit cell (twice the size of the primitive unit cell) at zero pressure is characterized by the lattice parameter sets ( $a=7.8306$  Å,  $b=4.6984$  Å, and  $c=4.6441$  Å) and ( $a=7.8142$  Å,  $b=4.7007$  Å, and  $c=4.6512$  Å) for the PBE and the PW91 functionals, respectively, with the eight atomic positions (8g Wyckoff positions):

$$\begin{aligned}
 &(x, y, \frac{1}{4}), \quad (x + \frac{1}{2}, y + \frac{1}{2}, \frac{1}{4}), \\
 &(\bar{x}, \bar{y}, \frac{3}{4}), \quad (\bar{x} + \frac{1}{2}, \bar{y} + \frac{1}{2}, \frac{3}{4}), \\
 &(\bar{x}, y, \frac{1}{4}), \quad (\bar{x} + \frac{1}{2}, y + \frac{1}{2}, \frac{1}{4}), \\
 &(x, \bar{y}, \frac{3}{4}), \quad (x + \frac{1}{2}, \bar{y} + \frac{1}{2}, \frac{3}{4}),
 \end{aligned}$$

with  $x=0.162\ 14$  and  $y=0.170\ 97$  for PBE and  $x=0.162\ 39$  and  $y=0.170\ 26$  for PW91. The cohesive energies at zero pressure are  $E_0=2.907$  and  $2.930$  eV per atom for the PBE and the PW91 functionals, respectively. To assess whether or not the predicted phase is metastable at zero pressure, we determine the Hessian matrix associated with a 144-atom supercell built based on the determined  $Cmcm$  symmetry. To this end we determine the force constants using an atomic displacement of  $0.015$  Å, followed by diagonalization. None of the eigenmodes are found to have negative eigenvalues, neither for PBE nor PW91, indicating the metastability of the predicted phase at zero pressure. Subsequently, we computed the elastic constants by measuring the stress tensor resulting from six independent cell distortions. The results, including the bulk modulus, are displayed in Table II and exhibit essentially equal outcomes for both functionals. A comparison of these results with the data in Table I shows that the predicted phase has a lower cohesive energy, is elastically softer, and has a larger atomic volume compared to  $\alpha$ -Ga. These results imply that, while the latter is the stable crystalline phase at zero external pressure, a transition into the predicted phase is conceivable at negative pressures as seen

in the classical MD simulations. To estimate the conditions under which this transition is expected to occur, we use the DFT data of the equilibrium cohesive energies, equilibrium volumes, and bulk moduli to compute the specific enthalpy,  $h=u+Pv$ , as a function of pressure at  $T=0$  K using the Rose universal equation of state<sup>23</sup> for both phases. The results indicate a transition pressure of  $P=-1.3$  GPa (for both functionals), below which the predicted structure becomes stable with respect to  $\alpha$ -Ga. From an experimental standpoint, such tensile conditions are accessible using modern growth and processing techniques,<sup>24</sup> allowing an experimental validation of this prediction. Moreover, the conjecture that the predicted phase is metastable even at zero pressure may further facilitate such verification.

The predicted and the  $\alpha$ -Ga phases show striking similarities from the structural point of view. The most captivating resemblance is the fact that each atom has only a single nearest neighbor, forming  $\text{Ga}_2$  dimers with essentially equal lengths of  $2.529$  and  $2.530$  Å for the predicted and the  $\alpha$ -Ga phases, respectively. In addition, in both phases each atom is further surrounded by six additional nearest-neighbor pairs at similar distances of  $2.713$ ,  $2.796$ , and  $2.823$  Å (predicted phase) and  $2.711$ ,  $2.769$ , and  $2.807$  Å ( $\alpha$ -Ga phase), respectively. The fact that these particular structural features are thought to be responsible for the mixed metallic-covalent character of the bonding in  $\alpha$ -Ga suggests that the electronic structure of the predicted phase may also be similar to that of  $\alpha$ -Ga. A comparison of the PBE electronic densities of states and the charge density plots depicted in Fig. 3(a) shows that this is indeed the case. The electronic densities of states of the two phases are essentially the same, both showing distinct pseudogaps at the Fermi level, which is indicative for the coexistence of metallic and covalent bonding characteristics.<sup>25</sup> Furthermore, the charge-density plots for both structures, depicted in Figs. 2(b) and 2(c), also show strong similarities, with a clear concentration of electronic charge between the pairs of atoms forming the Ga dimers. As shown in Fig. 3(b), however, the vibrational spectra exhibit pronounced deviations on the high-frequency end, which are related to the distinct disposition of the  $\text{Ga}_2$  dimers in both cases.

As a final point, we discuss the possibility of a connection between the present findings and the unknown metastable  $\epsilon$ -Ga phase observed in the phase-change experiments.<sup>1</sup> In this light, it is of interest to compare its cohesive energy to the other known metastable phases. The results are shown in Table III which contains the PBE and the PW91 cohesive energies of the  $\beta$ , the  $\gamma$ , the  $\delta$ , and the predicted phases at zero pressure. It is found that the predicted phase is the most strongly bound structure. In view of the fact that this struc-

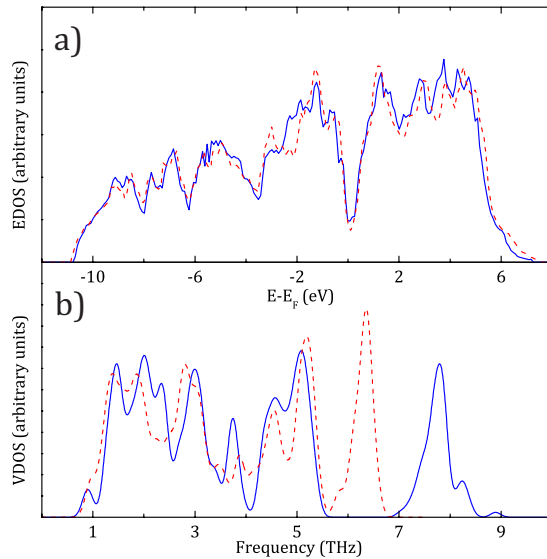


FIG. 3. (Color online) Comparison of (a) the electronic and (b) the vibrational densities of states of  $\alpha$ -Ga (dashed lines) and the predicted phase (full lines) for the PBE functional.

ture is predicted to be metastable at zero pressure, it is conceivable that it may in fact correspond to the unknown  $\epsilon$ -Ga phase. Unfortunately, however, given the lack of structural experimental information on the  $\epsilon$ -Ga phase, it is impossible to verify this possibility at present. In this context, experimental efforts directed toward unraveling the crystallographic structure of  $\epsilon$ -Ga and/or Ga phases at negative pressures are essential.

In summary, we present evidence for the existence of an

TABLE III. Comparison of DFT-GGA cohesive energies (in eV per atom) of different metastable phases of Ga for PW91 and PBE functionals at zero pressure.

	Predicted phase	$\beta$	$\gamma$	$\delta$
PBE	2.907	2.905	2.897	2.902
PW91	2.930	2.922	2.913	2.918

unknown crystalline form of elemental Ga. This finding, based on a combination of classical MD simulations and DFT calculations, extends our knowledge of the phase diagram of elemental Ga into the negative-pressure regime. The phase is characterized by  $Cmcm$  symmetry and, similar to the  $\alpha$ -Ga phase, features the presence of Ga dimers. As a consequence of this structural similarity, the electronic structure of the predicted phase is resemblance of that of  $\alpha$ -Ga, having a density of states with a pronounced pseudogap at the Fermi level. A comparison of the specific enthalpies of the predicted and the  $\alpha$ -Ga forms at  $T=0$  K suggests a transition pressure of  $-1.3$  GPa. Such tensile conditions are accessible using modern growth and processing techniques, allowing an experimental validation of this prediction. Moreover, the conjecture that the predicted phase is metastable even at zero pressure may further facilitate such verification. While it is conceivable that this structure corresponds to the unknown metastable  $\epsilon$ -Ga phase, the lack of experimental information regarding the latter precludes us, at present, to verify this possibility.

The work was supported by the Brazilian agencies FAPESP, CNPq, and CAPES. Part of the computations was carried out at CENAPAD-SP.

- <sup>1</sup>B. F. Soares, K. F. MacDonald, V. A. Fedotov, and N. I. Zheludev, *Nano Lett.* **5**, 2104 (2005).
- <sup>2</sup>W. Welnic, S. Botti, L. Reining, and M. Wuttig, *Phys. Rev. Lett.* **98**, 236403 (2007).
- <sup>3</sup>B. F. Soares, F. Jonsson, and N. I. Zheludev, *Phys. Rev. Lett.* **98**, 153905 (2007).
- <sup>4</sup>D. Lencer, M. Salinga, B. Grabowski, T. Hickel, J. Neugebauer, and M. Wuttig, *Nature Mater.* **7**, 972 (2008).
- <sup>5</sup>E. L. Gromnitskaya, O. F. Yagafarov, O. V. Stalgorova, V. V. Brazhkin, and A. G. Lyapin, *Phys. Rev. Lett.* **98**, 165503 (2007).
- <sup>6</sup>L. Bosio, *J. Chem. Phys.* **68**, 1221 (1978).
- <sup>7</sup>O. Degtyareva, M. I. McMahon, D. R. Allan, and R. J. Nelmes, *Phys. Rev. Lett.* **93**, 205502 (2004).
- <sup>8</sup>O. Schulte and W. B. Holzapfel, *Phys. Rev. B* **55**, 8122 (1997).
- <sup>9</sup>L. Bosio, A. Defrain, H. Curien, and A. Rimsky, *Acta Crystallogr., Sect. B: Struct. Crystallogr. Cryst. Chem.* **25**, 995 (1969).
- <sup>10</sup>L. Bosio, H. Curien, M. Dupont, and A. Rimsky, *Acta Crystallogr., Sect. B: Struct. Crystallogr. Cryst. Chem.* **29**, 367 (1973).
- <sup>11</sup>L. Bosio, H. Curien, M. Dupont, and A. Rimsky, *Acta Crystallogr., Sect. B: Struct. Crystallogr. Cryst. Chem.* **28**, 1974 (1972).

- <sup>12</sup>A. Defrain, *J. Chim. Phys. Phys.-Chim. Biol.* **74**, 851 (1977).
- <sup>13</sup>M. I. Baskes, S. P. Chen, and F. J. Cherne, *Phys. Rev. B* **66**, 104107 (2002).
- <sup>14</sup>S. Plimpton, *J. Comput. Phys.* **117**, 1 (1995).
- <sup>15</sup>M. Bernasconi, G. L. Chiarotti, and E. Tosatti, *Phys. Rev. B* **52**, 9988 (1995).
- <sup>16</sup>G. Kresse and J. Furthmüller, *Comput. Mater. Sci.* **6**, 15 (1996).
- <sup>17</sup>G. Kresse and J. Furthmüller, *Phys. Rev. B* **54**, 11169 (1996).
- <sup>18</sup>G. Kresse and D. Joubert, *Phys. Rev. B* **59**, 1758 (1999).
- <sup>19</sup>J. P. Perdew, K. Burke, and M. Ernzerhof, *Phys. Rev. Lett.* **77**, 3865 (1996).
- <sup>20</sup>J. P. Perdew and Y. Wang, *Phys. Rev. B* **45**, 13244 (1992).
- <sup>21</sup>R. W. G. Wyckoff, *Crystal Structures*, 2nd ed. (Wiley, New York, 1962), Vol. I.
- <sup>22</sup>E. A. Brandes, *Metals Reference Book* (Butterworths, London, 1983).
- <sup>23</sup>J. H. Rose, J. R. Smith, F. Guinea, and J. Ferrante, *Phys. Rev. B* **29**, 2963 (1984).
- <sup>24</sup>M. Wilson and P. F. McMillan, *Phys. Rev. Lett.* **90**, 135703 (2003).
- <sup>25</sup>V. Heine, *J. Phys. C* **1**, 222 (1968).